Identification of PEPT2 as an Important Candidate Molecule in 5-ALA-Mediated Fluorescence-Guided Surgery in WHO Grade II/III Gliomas

Chongxian Hou[1], Shigeru Yamaguchi[1], Yukitomo Ishi[1], Shunsuke Terasaka[1], Hiroyuki Kobayashi[1], Hiroaki Motegi[1], Kanako C. Hatanaka[2], Kiyohiro Houkin[1]

[1] Department of Neurosurgery and [2] Department of Surgical Pathology, Faculty of Medicine, Hokkaido University, Sapporo, Japan

Corresponding Author: Shigeru Yamaguchi, MD

Department of Neurosurgery, Faculty of Medicine, Hokkaido University

North 15 West 7, Kita-ku, Sapporo 060-8638, Japan

Phone: (+81)11-706-5987, Fax: (+81)11-708-7737

E-mail: yama-shu@med.hokudai.ac.jp

ORCID ID: 0000-0003-3710-5888

Abstract

Purpose: 5-aminolevulinic acid (5-ALA) fluorescence-guided surgery (FGS) appears to be a promising treatment for glioma. However, 5-ALA-mediated fluorescence cannot always be detected in grade II/III gliomas. We hypothesized that gene expression patterns in the Protoporphyrin IX (PpIX) synthesis pathway may be associated with intraoperative fluorescence status of grade II/III gliomas, and then attempted to identify the key molecule of 5-ALA-mediated fluorescence.

Methods: Using 50 surgically obtained specimens, which were diagnosed as grade II and III gliomas, we analyzed gene expression within the PpIX synthesis pathway to identify candidate molecules according to intraoperative 5-ALA-mediated fluorescence status. The most likely candidate gene was selected and confirmed by protein expression analysis. To evaluate the biological function of the molecule in PpIX synthesis, functional analysis was performed using specific, small interference (si)RNA in the SW-1783 human grade III glioma cell line.

Results: Among the genes involved in the porphyrin synthesis pathway, the mRNA expression of *Peptide transporter 2* (*PEPT2*) in FGS fluorescence-positive gliomas was significantly higher than that in fluorescence-negative gliomas. Protein expression of PEPT2 was also significantly higher in the fluorescence-positive gliomas, which was confirmed by western blot analysis and immunofluorescence analysis. The siRNA-mediated downregulation of the mRNA and protein expression of PEPT2 led to decreased PpIX fluorescence intensity, as confirmed by fluorescence spectrum analysis.

Conclusions: The results suggest PEPT2 is an important candidate molecule in 5-ALA-mediated FGS in grade II/III gliomas. As the overexpression of PEPT2 was associated with higher PpIX fluorescence intensity, PEPT2 may improve fluorescence-guided resection in grade II/III gliomas.

Key words: 5-aminolevulinic acid; Glioma; Fluorescence-guided surgery; Protoporphyrin IX

Introduction

Glioma is the most frequent primary intra-axial brain tumor. Surgery, combined with chemotherapy and radiotherapy, is the standard treatment; however, glioma remains incurable due to its high recurrence rate and invasiveness [1]. Patients with glioma can benefit from the maximum safest resection [2, 3]. However, surgeons often have difficulty distinguishing tumor tissue from normal tissue and in recognizing infiltrating glioma cells in normal tissues adjacent to tumor tissue intraoperatively. In addition, > 90% of recurrent gliomas occur within 2–3 cm of the borders of the original tumor lesion [4-7].

In recent years, 5-aminolevulinic acid (5-ALA) fluorescence-guided surgery (FGS) appears to be a promising treatment for glioma with documented survival benefits [8-10]. 5-ALA can be absorbed by glioma cells and then metabolized to Protoporphyrin IX (PpIX). Accumulated PpIX can lead to pronounced fluorescence when excited by violet–blue light, which assists in identifying the infiltrating area and increases the extent of tumor resection. However, the marginal region of tissue containing infiltrating glioma cells exhibits vague fluorescence due to insufficient PpIX accumulation [11]. In addition, 5-ALA-mediated fluorescence cannot be detected in all cases, particularly in the World Health Organization (WHO) grade II/III gliomas [12].

The molecular mechanisms underlying the accumulation of PpIX mediated by 5-ALA remain to be fully clarified. If the mechanisms can be elucidated, the fluorescence intensity mediated by 5-ALA in glioma may be managed by surgeons, and guide future maximum resection.

Compared with glioblastoma multiforme (GBM), a higher proportion of grade II/III cases do not exhibit 5-ALA-mediated fluorescence in tumor tissue. Therefore, the present study aimed to investigate the gene expression patterns of the PpIX synthesis pathway according to the 5-ALA-mediated

fluorescence status of grade II/III gliomas, and then identify the candidate molecules influencing the fluorescence.

Methods and materials

Surgical excision of glioma specimens

Since 2008, every patient who had suspected glioma in Hokkaido University Hospital (Sapporo, Japan) was administered with 5-ALA (20 mg/kg) orally 2–3 h prior to surgery. The fluorescence mediated by 5-ALA was visualized under a surgical microscope (OPMI-Pentero; Carl Zeiss) with high-powered, violet–blue LED light (CCS, Inc., Kyoto, Japan) during surgery. Surgically obtained glioma specimens emitting deep-red fluorescence or pink fluorescence were classified as fluorescence-positive. By contrast, glioma specimens without fluorescence were classified as fluorescence-negative. The fluorescence intensity status of each specimen was discussed and evaluated by two neurosurgeons (S.Y. and H.K.) during the procedure and recorded in the surgical records. If no fluorescence was detected in the tumor tissue, the tissue was cryopreserved and classified as fluorescence-negative. If fluorescence was partly detected in the excised tumor tissue, the fluorescing region was cryopreserved and the tissue was classified as fluorescence-positive. The surgical specimens were cryopreserved at -80˚C.

In the present study, surgical specimens from archives in neurosurgery department in Hokkaido University Hospital were selected according to the following criteria: (1) obtained at primary tumor resection without any adjuvant therapy, including chemotherapy or radiotherapy; (2) histologically diagnosed as grade II or III gliomas based on WHO 2007 criteria, which included diffuse astrocytoma, oligodendroglioma, oligoastrocytoma, anaplastic astrocytoma, anaplastic oligodendroglioma, and

anaplastic oligoastrocytoma; classification and pathologic diagnosis of gliomas were made by a certified pathologist; (3) cryopreserved tissue samples were assigned to a corresponding intraoperative fluorescence status. The mutation status of isocitrate dehydrogenase (IDH) was also investigated. Mutation hotspots at codon 132 of IDH1 and codon 172 of IDH2 were screened using Sanger sequencing. In addition, 1p/19q loss of heterozygosity status was analyzed using a multiplex ligation-dependent probe amplification procedure. The tumors were re-diagnosed according to the WHO 2016 criteria according to the IDH and 1p19q status. In addition, all patients received magnetic resonance imaging (MRI) with contrast enhancement preoperatively. According to the enhancement pattern, the tumors were classified as enhanced tumors and non-enhanced tumors. Tumors that exhibited apparent enhancement, including a heterogeneous or ring-like pattern, were defined as an enhanced tumor. Tumors without obvious enhancement were defined as a non-enhanced tumor.

Quantitative real-time polymerase chain reaction (qPCR) analysis

As a control reference, two sets of commercially available human brain total RNA were obtained (Life Technologies; Clontech). The glioma total RNA was extracted from the frozen specimens using an All Prep DNA/RNA Mini kit (QIAGEN) based on the manufacturer's instructions. cDNA was synthesized from total RNA using the PrimeScript™ II 1st Strand cDNA Synthesis kit (Takara Biotechnology Co., Ltd., Dalian, China). Several genes within the PpIX synthesis pathway were selected, including *ALAD, ALAS1, ABCG2, ABCB6, CPOX, FECH, HO-1, PEPT2,* and *UROS,* to identify candidate molecules in 5-ALA-mediated grade II/III glioma fluorescence. The gene primers are listed in Table S1. Reverse transcription-qPCR analysis was performed with LightCycler 96 (Roche Diagnostics, Basel, Switzerland) and the PCR product specificities were confirmed via melt curve

analysis. To normalize the target transcript, *GAPDH* was used, which is one of the most stably expressed housekeeping genes for endogenous control. The PCR experiments were run in triplicate. The -ΔΔCT equation was applied to calculate the relative expression of tumor samples with the average value of the normal brain as a reference control.

Immunofluorescence analysis.

The protein expression of PEPT2 was detected by immunofluorescence staining using the paraffin-embedded tumor sections. The sections were incubated with rabbit polyclonal PEPT2 antibody (Abcam, 1:100) as the primary antibody in 0.5% BSA for 1 h at room temperature. Phosphate-buffered saline (PBS) was used in the negative control instead of the primary antibody. Alexa Fluor® 594 goat anti-rabbit antibody (Life Technologies, 1:200) in 0.5% BSA was used as the secondary antibody. The nuclei were stained with DAPI (Invitrogen). Staining was observed using the KEYENCE BZ-X700 fluorescence microscope with a 20X objective.

Western blot analysis

The proteins were extracted from five fluorescence-negative grade II/III gliomas and five fluorescence-positive grade II/III gliomas. The proteins were loaded on a Blot™ 4%–12% Bis–Tris Plus gel (Invitrogen™), electrophoresed, and fractionated at 200 V for 30 min in SDS running buffer, and then transferred onto a 0.2-μm-pore nitrocellulose membrane (Invitrogen™). Following blocking with 2% ECL Prime blocking agent (GE Healthcare) in PBS-Tween 20 for 1 h at room temperature, the membrane was incubated with primary antibodies against PEPT2 (Abcam,1:500) and β-actin (Santa Cruz Biotechnology, Inc., 1:1,000) with gentle shaking at 4˚C overnight, followed by incubation with a

horseradish peroxidase-conjugated, goat anti-mouse secondary antibody (Santa Cruz Biotechnology, Inc., 1:5,000) or goat anti-rabbit secondary antibody (Santa Cruz Biotechnology, Inc., 1:5,000) at room temperature for 2 h. Finally, the proteins were visualized using the enhanced chemiluminescence method (Bio-Rad Laboratories, Inc., Hercules, CA, USA).

RNA interference experiments

The commercially available SW-1783 human grade III glioma cell line (ATCC®) was used in the present study. The SW-1783 cells were maintained in DMEM-high glucose (NacalaiTesque), supplemented with 10% fetal bovine serum (FBS, Life Technologies), in a 5% CO_2-humidified incubator at 37˚C. The SW-1783 cells were plated in 6-well plates. Each well of cells was transfected with 2,500 ng of *PEPT2* Silencer® Select Pre-designed small interfering (si)RNA (cat. no. s13065, Life Technologies) or Silencer® Select Negative Control #1 siRNA (Life Technologies) using Lipofectamine 3000 (Invitrogen™) according to the manufacturer's instructions. The cells were harvested 24 h following transfection and subjected to RT-qPCR and western blot analyses to examine the silencing efficiency.

PpIX fluorescence spectrum analysis

The cells were randomly divided into four groups: Negative control (NC) siRNA, NC siRNA + 5ALA, PEPT2 siRNA, and PEPT2 siRNA + 5ALA. The 5-ALA (Cosmo Bio) was stored at 4˚C in the dark and dissolved in DMEM-high glucose (NacalaiTesque), supplemented with 10% FBS, to a final concentration of 200 μg/ml. For the NC + 5ALA group and the PEPT2 siRNA + 5ALA group, the culture medium was replaced with a medium containing 5-ALA 24 h following transfection, followed

by incubation for 4 h at 37˚C. For the NC siRNA group and PEPT2 siRNA group, the culture medium was replaced with fresh DMEM-high glucose, supplemented with 10% FBS without 5-ALA, at 24 h post-transfection. Following incubation for 4 h, the cells were washed with PBS (NacalaiTesque) and collected using 0.05% trypsin with 0.5 mM ethylenediaminetetraacetic acid in 15-mL conical tubes (FALCON®). The liquid supernatant was discarded following centrifugation at 1,000 revolutions per min. The fluorescence spectrum was detected by VLD-EX (SBI Pharma) in the dark room. Subsequently, the illuminant with optical fiber was placed into the 15-mL conical tubes. The distance between the bottom of the conical tube and the illuminant was maintained at ~2 cm. The excitation wavelength was 406 nm. Visual images were captured using a camera (ILCE-A5000, Sony). The quantified fluorescence spectrum was presented on the screen of the VLD-EX machine.

Statistical analysis

SPSS 22.0 and R statistical software, version 3.4.1, were used to conduct all statistical analyses. Continuous variables were compared using the one-way analysis of variance. The Least Significant Difference test was used to compare differences between groups. Categorical variables are expressed as frequency (percentage) and were compared using the Chi-square ($\chi 2$) test. $P < 0.05$ was considered to indicate a statistically significant difference. Hierarchical clustering analysis, presented as a heat map, was performed using R software to demonstrate the distinguishable mRNA expression profiles among the samples. “hclust” was used to compute the hierarchical clustering analysis, with the Ward method as the method of clustering, and the Euclidean distance as the distance metric. The results were visualized using dendrograms and heatmaps.

Results

Patient characteristics

A total of 50 grade II/III glioma specimens, including grade II (N = 22) and grade III (N = 28) specimens, were matched to the above criteria. The tumors were re-diagnosed according to the WHO 2016 criteria. The types and the numbers of the grade II and grade III gliomas are listed in Table S2. The numbers of cases in terms of the grade of the glioma and 5-ALA-mediated fluorescence status are listed in Table 1. In the grade II gliomas, only 2/22 cases (9%) were detected with fluorescence. By contrast, in the grade III gliomas, 19/28 cases (68%) were detected with fluorescence and 9 cases (32%) showed no fluorescence. The fluorescence status was significantly influenced by histological malignancy ($p<0.001$). The correlation between IDH status and 5-ALA-mediated fluorescence status is shown in Table 2. Gliomas with IDH mutations were predominantly fluorescence-negative (25/36 cases; 69%), whereas gliomas without IDH mutations were predominantly fluorescence-positive (10/14 cases; 71%). The difference was statistically significant ($p = 0.009$). The correlations between MRI contrast enhance status and the 5-ALA-mediated fluorescence status of the tumors are shown in Table S3. The non-enhanced tumors were predominantly fluorescence-negative (23/34 cases; 68%), and the difference was statistically significant ($p = 0.044$).

mRNA expression of genes in the PpIX synthesis pathway

The relative mRNA expression levels, according to 5-ALA-mediated fluorescence status, are shown in Fig. 1a. Compared with those in the normal brain, the mRNA expression of levels of *ABCG2* ($p < 0.05$), *ABCB6* ($p < 0.05$), and *HO-1* ($p < 0.05$) were significantly higher in the fluorescence-negative grade II/III gliomas, and the mRNA expression levels of *PEPT2* ($p < 0.05$),

ABCG2 ($p < 0.01$), *ABCB6* ($p < 0.01$), and *HO-1* ($p < 0.001$) were significantly higher in the fluorescence-positive grade II/III gliomas. Compared with the fluorescence-negative grade II/III gliomas, the mRNA expression levels of *PEPT2* ($p < 0.05$), *ALAD* ($p < 0.01$), *ABCG2* ($p < 0.05$), *ABCB6* ($p < 0.01$), *CPOX* ($p < 0.05$), *HO-1* ($p < 0.05$), and *UROS* ($p < 0.001$) were also significantly higher in the fluorescence-positive gliomas. There were no significant differences in the mRNA expression of *ALAS1* or *FECH* between the groups.

According to the PpIX synthesis pathway (Fig. 1b), PEPT2 is responsible for transporting 5-ALA and PEPT2 is an upstream molecule in the PpIX synthesis pathway. Therefore, the data obtained suggested that the overexpression of PEPT2 affected the fluorescence intensity mediated by 5-ALA in grade II/III gliomas. In the IDH mutant specimens, the mRNA expression levels in the PpIX synthesis pathway were similar in all grade II/III gliomas (Fig. S1a). The IDH wild-type grade II/III gliomas also exhibited similar mRNA expression tendency (Fig. S1b). The present study also compared the mRNA expression of *PEPT2* between MRI enhanced grade II/III gliomas and MRI non-enhanced grade II/III gliomas. The mRNA expression of *PEPT2* in the enhanced tumors was higher than that in the non-enhanced tumors, although this difference did not reach statistical significance (data not shown).

Hierarchical clustering of the expression patterns demonstrated there are two major clusters (Fig. 1c). Cluster 1 contained 19 tumors, and cluster 2 contained 31 tumors. In terms of the 5-ALA-mediated fluorescence status, the majority of fluorescence-negative tumors (16/28 tumors; 57%) and three of the 21 fluorescence-positive tumors (14%) belonged to cluster 1. The majority of the fluorescence-positive tumors (18/21 tumors; 86%) belonged to cluster 2. In addition, in terms of the IDH status, only one out of the 14 IDH mutant gliomas (7%) belonged to cluster 1. In terms of MRI contrast enhancement status, only one of the 16 MRI contrast enhanced tumors (6%) belonged to cluster 1.

Protein expression of PEPT2 measured by immunofluorescence and western blot analysis

According to the results of the RT-qPCR analysis of the PpIX synthesis pathway, the present study focused on the overexpression of PEPT2, as it may be important in the accumulation of PpIX following the administration of 5-ALA in grade II/III gliomas. PEPT2, also known as SLC15A2, is widely expressed in glial cells and mediates the uptake of peptide substrates. PEPT2 polyclonal antibody was used to detect protein expression by immunofluorescence in five fluorescence-positive grade II/III gliomas and five fluorescence-negative grade II/III gliomas. The results of the protein expression of PEPT2 are shown in Fig. 2a. The immunofluorescence results of three fluorescence-positive cases and three fluorescence-negative cases are shown in Fig. 2a. Compared with the fluorescence-negative grade II/III gliomas, a higher expression of PEPT2 was presented in the fluorescence-positive grade II/III gliomas.

The present study also investigated the relative protein expression levels of PEPT2 and compared them between five fluorescence-negative grade II/III gliomas and five fluorescence-positive grade II/III gliomas using western blot analysis. Consistent with the product datasheet of primary PEPT2 antibody, bands at a size of 90 kDa were observed, and the predicted band was identified at a size of 82 kDa. The results (Fig. 2b, c) demonstrated that the protein expression of PEPT2 in the fluorescence-positive grade II/III gliomas was significantly higher than that in the fluorescence-negative grade II/III gliomas ($p < 0.01$). These results revealed that the overexpression of PEPT2 might be important in the 5-ALA-mediated PpIX fluorescence intensity of gliomas.

RNA interference and PpIX fluorescence spectrum analysis.

In order to further confirm the exact function of PEPT2, the present study aimed to inhibit the expression of PEPT2 in the SW-1783 cell line using siRNA. PEPT2 mRNA and protein expression was successfully downregulated by ~50% at 24 h post-transfection with specific siRNA (Fig. 3a–c). The fluorescence spectrums of the four groups (NC siRNA + 5ALA, NC siRNA, PEPT2 siRNA + 5ALA, and PEPT2 siRNA) were detected using VLD-EX in the dark room. The peak wavelength of 636 nm represents the PpIX fluorescence spectrum. The results demonstrated that the downregulation of PEPT2 led to decreased fluorescence intensity (Fig. 3d, e) in the SW-1783 cells. This result suggested that 5-ALA-mediated fluorescence may be influenced by the expression of PEPT2 in grade II/III gliomas.

Discussion

Patients with glioma may benefit from the maximum safe tumor resection [2,3]. However, surgeons may have difficulty distinguishing tumor tissue from normal tissue during surgery. 5-ALA-mediated FGS has become a useful surgical technique in glioma resection and improves the overall survival of patients with malignant glioma [8-10]. However, fluorescence cannot be detected in all cases of glioma, particularly in grade II/III tumors [12]. In the present study, in the grade II gliomas, only 2/22 cases (9%) were detected with fluorescence. By contrast, in the grade III gliomas, 19/28 cases (68%) were detected with fluorescence and 9 cases (32%) showed no fluorescence (Table 1). Therefore, the 5-ALA-mediated FGS in grade II/III gliomas may be useful.

The FGS mechanism mediated by 5-ALA in gliomas remains to be fully elucidated. In particular, compared with GBMs, there has been no previous investigation of the molecular mechanism underlying 5-ALA-mediated FGS in grade II/III glioma. Fluorescence-positive and

fluorescence-negative cases may show different gene expression patterns. Therefore, the present study was performed to investigate the differences in gene expression patterns between fluorescence-positive grade II/III gliomas and fluorescence-negative grade II/III gliomas. If the underlying genetic mechanism of the fluorescence of PpIX mediated by 5-ALA can be clarified, the fluorescence intensity may be managed by neurosurgeons in the future.

The present study first attempted to identify candidate genes with an effect on 5-ALA-mediated PpIX fluorescence intensity. The mRNA expression levels of genes in the PpIX synthesis pathway were compared among normal brain tissues, fluorescence-negative grade II/III gliomas, and fluorescence-positive grade II/III gliomas. The results demonstrated that mRNA expression levels of *ALAD* ($p < 0.01$), *ABCG2* ($p < 0.05$), *ABCB6* ($p < 0.01$), *CPOX* ($p < 0.05$), *HO-1* ($p < 0.05$), *PEPT2* ($p < 0.05$), and *UROS* ($p < 0.001$) were significantly higher in the fluorescence-positive grade II/III gliomas than the fluorescence-negative grade II/III gliomas (Fig. 1a).

Among the above candidate genes, the present study focused on PEPT2 as it is an upstream molecule in the PpIX synthesis pathway (Fig. 1b). In the central nervous system (CNS), PEPT2 can remove peptide/mimetic drugs from the cerebrospinal fluid to the plasma. PEPT2 is also responsible for the uptake of peptide/mimetic drugs from brain extracellular fluid into brain cells, which is important in regulating drug metabolism in the CNS [13-15].

PEPT2 protein consists of 729 amino acids, and the core molecular size is 81,940 Da. PEPT2 is a high-affinity and low-capacity transporter, which is widely expressed in the brain, lung, kidney, eye, and mammary gland [16, 17]. PEPT2 is located in the cell membrane and is responsible for the selective transportation of peptides, amino acids, and drugs [18-20]. PEPT1 and PEPT2 are responsible for 5-ALA uptake. However, the affinity of PEPT2 to the same substrates is higher than that of PEPT1,

which is mainly expressed in the intestine [21, 22]. In general, > 400 dipeptides and 8,000 tripeptides, including 20 essential L-α-amino acids and the majority of D-enantiomers, can be sequence-independently transported by PEPT2. In addition, numerous peptide-like drugs, including β-lactam antibiotics, angiotensin-converting enzyme inhibitors, and peptidase inhibitors can be mediated and transported by PEPT2 substrate [18, 20, 23].

Previous functional investigations of PEPT2 have focused predominantly on its transportation and absorption effect. In the kidney, PEPT2 is almost entirely responsible for the reabsorption of peptides and peptidomimetics [18, 23-25]. PEPT2 in the lung is located in alveolar type II pneumocytes, the bronchial epithelium, and the endothelium of small vessels, and is responsible for delivering peptides and peptidomimetics [26, 27]. Of note, it has been demonstrated that PEPT2-null mice are fertile and healthy. Therefore, the exact function of PEPT2 requires further investigation [28, 29].

In the present study, it was hypothesized that PEPT2 may be key in the uptake of 5-ALA and 5-ALA-mediated PpIX fluorescence in grade II/III gliomas. The protein expression of PEPT2 was compared between fluorescence-negative grade II/III gliomas and fluorescence-positive grade II/III gliomas. The results demonstrated that the protein expression of PEPT2 in fluorescence-positive grade II/III gliomas was significantly higher than that in fluorescence-negative grade II/III gliomas ($p < 0.05$), which suggested that the levels of PEPT2 may affect the fluorescence intensity of PpIX. To further investigate the exact function of PEPT2, the mRNA and protein expression of PEPT2 were inhibited in a grade III glioma cell line and the PpIX fluorescence spectrum was detected. The results demonstrated that the downregulation of PEPT2 decreased fluorescence intensity. These findings suggest that the expression of PEPT2 is important for the 5-ALA-mediated fluorescence intensity of PpIX.

Previous studies have demonstrated that the overexpression of ABCB6 can enhance the

5-ALA-mediated fluorescence of PpIX in human glioma [30]. ABCB6 is a transporter in the PpIX metabolic pathway. This result is consistent with the RT-qPCR results in the present study, which showed that the mRNA of *ABCB6* was overexpressed in fluorescence-positive grade II/III gliomas. In a study conducted by Takahashi *et al* [31], the mRNA expression levels of *PEPT2*, *ABCB6*, *and ABCG2* appeared to be relatively lower in samples with a high level of fluorescence, which is inconsistent with the results of the present study. This may be due to the samples used in the previous study being glioblastomas and metastatic brain tumors, which may exhibit gene expression patterns distinct from those of grade II/III gliomas. Hu e*t al* [32] found that PEPT2 reduced the neurotoxicity of 5-ALA, which indicates that the expression of PEPT2 may also influence the efficacy of 5-ALA-mediated photodynamic therapy. This also suggests that PEPT2 is important in glioma treatment. Therefore, future studies may examine the role of PEPT2 in glioma photodynamic therapy.

In conclusion, the present study is the first, to the best of our knowledge, to demonstrate that PEPT2 is an important gene/protein in 5-ALA-mediated FGS in grade II/III gliomas. The overexpression of PEPT2 was associated with a higher fluorescence intensity of PpIX in grade II/III gliomas. These results may provide clues to improve the surgical treatment of grade II/III gliomas in the future.

Acknowledgement This study was supported by Grant-in-Aid for Young Scientists (B) (KAKENHI; grant no. 16K19991). The authors would like to thank Enago (www.enago.jp) for the English language review.

Compliance with Ethical Standards

Conflict of interest

The authors declare no conflict of interest.

Ethical approval

This study was approved by the local Ethics Committee at Hokkaido University Hospital (Sapporo, Japan; 017-0032). All procedures performed in the present study were in accordance with 1964 Helsinki Declaration and its later amendments.

References

1. Stupp R, Mason WP, van den Bent MJ, Weller M, Fisher B, Taphoorn MJ, Belanger K, Brandes AA, Marosi C, Bogdahn U, Curschmann J, Janzer RC, Ludwin SK, Gorlia T, Allgeier A, Lacombe D, Cairncross JG, Eisenhauer E, Mirimanoff RO, European Organisation for R, Treatment of Cancer Brain T, Radiotherapy G, National Cancer Institute of Canada Clinical Trials G (2005) Radiotherapy plus concomitant and adjuvant temozolomide for glioblastoma. The New England journal of medicine 352: 987-996 doi:10.1056/NEJMoa043330

2. Lacroix M, Abi-Said D, Fourney DR, Gokaslan ZL, Shi W, DeMonte F, Lang FF, McCutcheon IE, Hassenbusch SJ, Holland E, Hess K, Michael C, Miller D, Sawaya R (2001) A multivariate analysis of 416 patients with glioblastoma multiforme: prognosis, extent of resection, and survival. Journal of neurosurgery 95: 190-198 doi:10.3171/jns.2001.95.2.0190

3. Sanai N, Berger MS (2008) Glioma extent of resection and its impact on patient outcome. Neurosurgery 62: 753-764; discussion 264-756 doi:10.1227/01.neu.0000318159.21731.cf

4. Aydin H, Sillenberg I, von Lieven H (2001) Patterns of failure following CT-based 3-D irradiation for malignant glioma. Strahlentherapie und Onkologie : Organ der Deutschen Rontgengesellschaft [et al] 177: 424-431

5. Clarke J, Butowski N, Chang S (2010) Recent advances in therapy for glioblastoma. Archives of neurology 67: 279-283 doi:10.1001/archneurol.2010.5

6. Theeler BJ, Groves MD (2011) High-grade gliomas. Current treatment options in neurology 13: 386-399 doi:10.1007/s11940-011-0130-0

7. Wallner KE, Galicich JH, Krol G, Arbit E, Malkin MG (1989) Patterns of failure following treatment for glioblastoma multiforme and anaplastic astrocytoma. International journal of

radiation oncology, biology, physics 16: 1405-1409

8. Aldave G, Tejada S, Pay E, Marigil M, Bejarano B, Idoate MA, Diez-Valle R (2013) Prognostic value of residual fluorescent tissue in glioblastoma patients after gross total resection in 5-aminolevulinic Acid-guided surgery. Neurosurgery 72: 915-920; discussion 920-911 doi:10.1227/NEU.0b013e31828c3974

9. Stummer W, Pichlmeier U, Meinel T, Wiestler OD, Zanella F, Reulen HJ, Group AL-GS (2006) Fluorescence-guided surgery with 5-aminolevulinic acid for resection of malignant glioma: a randomised controlled multicentre phase III trial. The Lancet Oncology 7: 392-401 doi:10.1016/S1470-2045(06)70665-9

10. Stummer W, Stocker S, Wagner S, Stepp H, Fritsch C, Goetz C, Goetz AE, Kiefmann R, Reulen HJ (1998) Intraoperative detection of malignant gliomas by 5-aminolevulinic acid-induced porphyrin fluorescence. Neurosurgery 42: 518-525; discussion 525-516

11. Utsuki S, Oka H, Sato S, Suzuki S, Shimizu S, Tanaka S, Fujii K (2006) Possibility of using laser spectroscopy for the intraoperative detection of nonfluorescing brain tumors and the boundaries of brain tumor infiltrates. Technical note. Journal of neurosurgery 104: 618-620 doi:10.3171/jns.2006.104.4.618

12. Jaber M, Wolfer J, Ewelt C, Holling M, Hasselblatt M, Niederstadt T, Zoubi T, Weckesser M, Stummer W (2016) The Value of 5-Aminolevulinic Acid in Low-grade Gliomas and High-grade Gliomas Lacking Glioblastoma Imaging Features: An Analysis Based on Fluorescence, Magnetic Resonance Imaging, 18F-Fluoroethyl Tyrosine Positron Emission Tomography, and Tumor Molecular Factors. Neurosurgery 78: 401-411; discussion 411 doi:10.1227/NEU.0000000000001020

13. Chen X, Keep RF, Liang Y, Zhu HJ, Hammarlund-Udenaes M, Hu Y, Smith DE (2017) Influence of peptide transporter 2 (PEPT2) on the distribution of cefadroxil in mouse brain: A microdialysis study. Biochemical pharmacology 131: 89-97 doi:10.1016/j.bcp.2017.02.005

14. Hu Y, Ocheltree SM, Xiang J, Keep RF, Smith DE (2005) Glycyl-L-glutamine disposition in rat choroid plexus epithelial cells in primary culture: role of PEPT2. Pharmaceutical research 22: 1281-1286 doi:10.1007/s11095-005-5261-0

15. Novotny A, Xiang J, Stummer W, Teuscher NS, Smith DE, Keep RF (2000) Mechanisms of 5-aminolevulinic acid uptake at the choroid plexus. Journal of neurochemistry 75: 321-328

16. Daniel H, Kottra G (2004) The proton oligopeptide cotransporter family SLC15 in physiology and pharmacology. Pflugers Archiv: European journal of physiology 447: 610-618 doi:10.1007/s00424-003-1101-4

17. Liu W, Liang R, Ramamoorthy S, Fei YJ, Ganapathy ME, Hediger MA, Ganapathy V, Leibach FH (1995) Molecular cloning of PEPT 2, a new member of the H+/peptide cotransporter family, from human kidney. Biochimica et biophysica acta 1235: 461-466

18. Rubio-Aliaga I, Daniel H (2002) Mammalian peptide transporters as targets for drug delivery. Trends in pharmacological sciences 23: 434-440

19. Terada T, Inui K (2004) Peptide transporters: structure, function, regulation and application for drug delivery. Current drug metabolism 5: 85-94

20. Terada T, Saito H, Sawada K, Hashimoto Y, Inui K (2000) N-terminal halves of rat H+/peptide transporters are responsible for their substrate recognition. Pharmaceutical research 17: 15-20

21. Doring F, Walter J, Will J, Focking M, Boll M, Amasheh S, Clauss W, Daniel H (1998) Delta-aminolevulinic acid transport by intestinal and renal peptide transporters and its

physiological and clinical implications. The Journal of clinical investigation 101: 2761-2767 doi:10.1172/JCI1909

22. Wang M, Zhang X, Zhao H, Wang Q, Pan Y (2010) Comparative analysis of vertebrate PEPT1 and PEPT2 genes. Genetica 138: 587-599 doi:10.1007/s10709-009-9431-6

23. Verrey F, Singer D, Ramadan T, Vuille-dit-Bille RN, Mariotta L, Camargo SM (2009) Kidney amino acid transport. Pflugers Archiv: European journal of physiology 458: 53-60 doi:10.1007/s00424-009-0638-2

24. Sala-Rabanal M, Loo DD, Hirayama BA, Wright EM (2008) Molecular mechanism of dipeptide and drug transport by the human renal H+/oligopeptide cotransporter hPEPT2. American journal of physiology Renal physiology 294: F1422-1432 doi:10.1152/ajprenal.00030.2008

25. Shen H, Ocheltree SM, Hu Y, Keep RF, Smith DE (2007) Impact of genetic knockout of PEPT2 on cefadroxil pharmacokinetics, renal tubular reabsorption, and brain penetration in mice. Drug metabolism and disposition: the biological fate of chemicals 35: 1209-1216 doi:10.1124/dmd.107.015263

26. Groneberg DA, Nickolaus M, Springer J, Doring F, Daniel H, Fischer A (2001) Localization of the peptide transporter PEPT2 in the lung: implications for pulmonary oligopeptide uptake. The American journal of pathology 158: 707-714 doi:10.1016/S0002-9440(10)64013-8

27. Gukasyan HJ, Uchiyama T, Kim KJ, Ehrhardt C, Wu SK, Borok Z, Crandall ED, Lee VHL (2017) Oligopeptide Transport in Rat Lung Alveolar Epithelial Cells is Mediated by Pept2. Pharmaceutical research 34: 2488-2497 doi:10.1007/s11095-017-2234-z

28. Frey IM, Rubio-Aliaga I, Klempt M, Wolf E, Daniel H (2006) Phenotype analysis of mice deficient in the peptide transporter PEPT2 in response to alterations in dietary protein intake.

Pflugers Archiv: European journal of physiology 452: 300-306 doi:10.1007/s00424-005-0042-5

29. Rubio-Aliaga I, Frey I, Boll M, Groneberg DA, Eichinger HM, Balling R, Daniel H (2003) Targeted disruption of the peptide transporter Pept2 gene in mice defines its physiological role in the kidney. Molecular and cellular biology 23: 3247-3252

30. Zhao SG, Chen XF, Wang LG, Yang G, Han DY, Teng L, Yang MC, Wang DY, Shi C, Liu YH, Zheng BJ, Shi CB, Gao X, Rainov NG (2013) Increased expression of ABCB6 enhances protoporphyrin IX accumulation and photodynamic effect in human glioma. Annals of surgical oncology 20: 4379-4388 doi:10.1245/s10434-011-2201-6

31. Takahashi K, Ikeda N, Nonoguchi N, Kajimoto Y, Miyatake S, Hagiya Y, Ogura S, Nakagawa H, Ishikawa T, Kuroiwa T (2011) Enhanced expression of coproporphyrinogen oxidase in malignant brain tumors: CPOX expression and 5-ALA-induced fluorescence. Neuro-oncology 13: 1234-1243 doi:10.1093/neuonc/nor116

32. Hu Y, Shen H, Keep RF, Smith DE (2007) Peptide transporter 2 (PEPT2) expression in brain protects against 5-aminolevulinic acid neurotoxicity. Journal of neurochemistry 103: 2058-2065 doi:10.1111/j.1471-4159.2007.04905.x

Figure legends

Fig. 1 Relative mRNA expression levels, PpIX/heme biosynthesis, and metabolism pathway, hierarchical clustering of the expression patterns. **a** Relative mRNA expression levels of *ALAS1*, *ALAD*, *ABCG2*, *ABCB6*, *CPOX*, *FECH*, *HO-1*, *PEPT2*, and *UROS* of all grade II/III gliomas in three groups. Data are presented as the mean ± standard error of the mean with three replicates for each glioma specimen. #P < 0.05 compared with the normal brain group, ##P < 0.01 compared with the normal brain group, ###P < 0.001 compared with the normal brain group, *P < 0.05 compared with the fluorescence-negative group, **P < 0.01 compared with the fluorescence-negative group, *** P < 0.001 compared with the fluorescence-positive group. **b** PpIX/heme biosynthesis and metabolic pathway. Multiple enzymes and transporters are involved in this pathway. The enzymes are marked with rectangles. **c** Heatmap summary and hierarchical clustering for *ALAD*, *ALAS1*, *ABCG2*, *ABCB6*, *CPOX*, *FECH*, *HO-1*, *PEPT2*, and *UROS* of the 50 specimens. Samples are depicted in rows and RNAs are depicted in columns. Red indicates high expression, and green indicates low expression. ABCB10, ATP binding cassette subfamily B member 10; ABCC1, 2 or 3, ATP binding cassette subfamily C member 1, 2 or 3; PBzR, peripheral benzodiazepine receptor; FLVCR1, feline leukemia virus subgroup c receptor 1; SLC25A38, solute carrier family 25 member 38.

Fig. 2 Protein expression of PEPT2 measured by immunofluorescence analysis and western blot analysis. **a** Protein expression of PEPT2 measured by immunofluorescence analysis. PBS was used in negative control instead of primary antibody. PEPT2 protein was detected with Alexa Fluor® 594 goat anti-rabbit secondary antibody (red). Nuclei were stained with DAPI (blue). Protein expression of PEPT2 in fluorescence-positive grade II/III gliomas was higher than in fluorescence-negative grade

II/III gliomas. **b** Western blotting of five fluorescence-positive grade II/III gliomas and five fluorescence-negative grade II/III gliomas using antibody against PEPT2. β-actin was used as a loading control. **c** Comparison of relative protein expression levels of PEPT2 between five fluorescence-positive grade II/III gliomas and five fluorescence-negative grade II/III gliomas based on densitometric analysis of western blots. Data are presented as the mean ± standard error of the mean of three replicates for each glioma specimen. *$p<0.05$ compared with the fluorescence-negative grade II/III gliomas.

Fig. 3 RNA interference experiments and PpIX fluorescence spectrum analysis. **a** Western blotting of SW-1783 cells transfected with PEPT2 siRNA or negative control siRNA using antibody against PEPT2. β-actin was used as a loading control. **b** Semi-quantitative analysis of western blots. Data are presented as the mean ± standard error of the mean of three replicates for each experimental condition. **c** mRNA expression of *PEPT2* in SW-1783 cells transfected with PEPT2 siRNA or negative control siRNA. **$p<0.01$ compared with SW-1783 cells transfected with negative control siRNA. **d** PpIX fluorescence spectrum of the four groups (NC siRNA + 5ALA, NC siRNA, PEPT2 siRNA + 5ALA, and PEPT2 siRNA). **e** Visual images of the fluorescence of PpIX in the four groups. The density of cells in each sample was ~$1x10^6$.

Table 1. 5-ALA-mediated FGS fluorescence status in relation to the grading of grade II/III gliomas.

Fluorescence status	Grade II glioma	Grade III glioma	Total
Fluorescence-positive	2	19	21
Fluorescence-negative	20	9	29
Total	22	28	50

5-ALA, 5-aminolevulinic acid; FGS, fluorescence-guided surgery.

490 Table 2. 5-ALA-mediated fluorescence status in relation to the IDH status of 50 grade II/III gliomas.

Fluorescence status	IDH mutant glioma	IDH wild-type glioma	Total
Fluorescence-positive	11	10	21
Fluorescence-negative	25	4	29
Total	36	14	50

491 5-ALA, 5-aminolevulinic acid; IDH, isocitrate dehydrogenase.

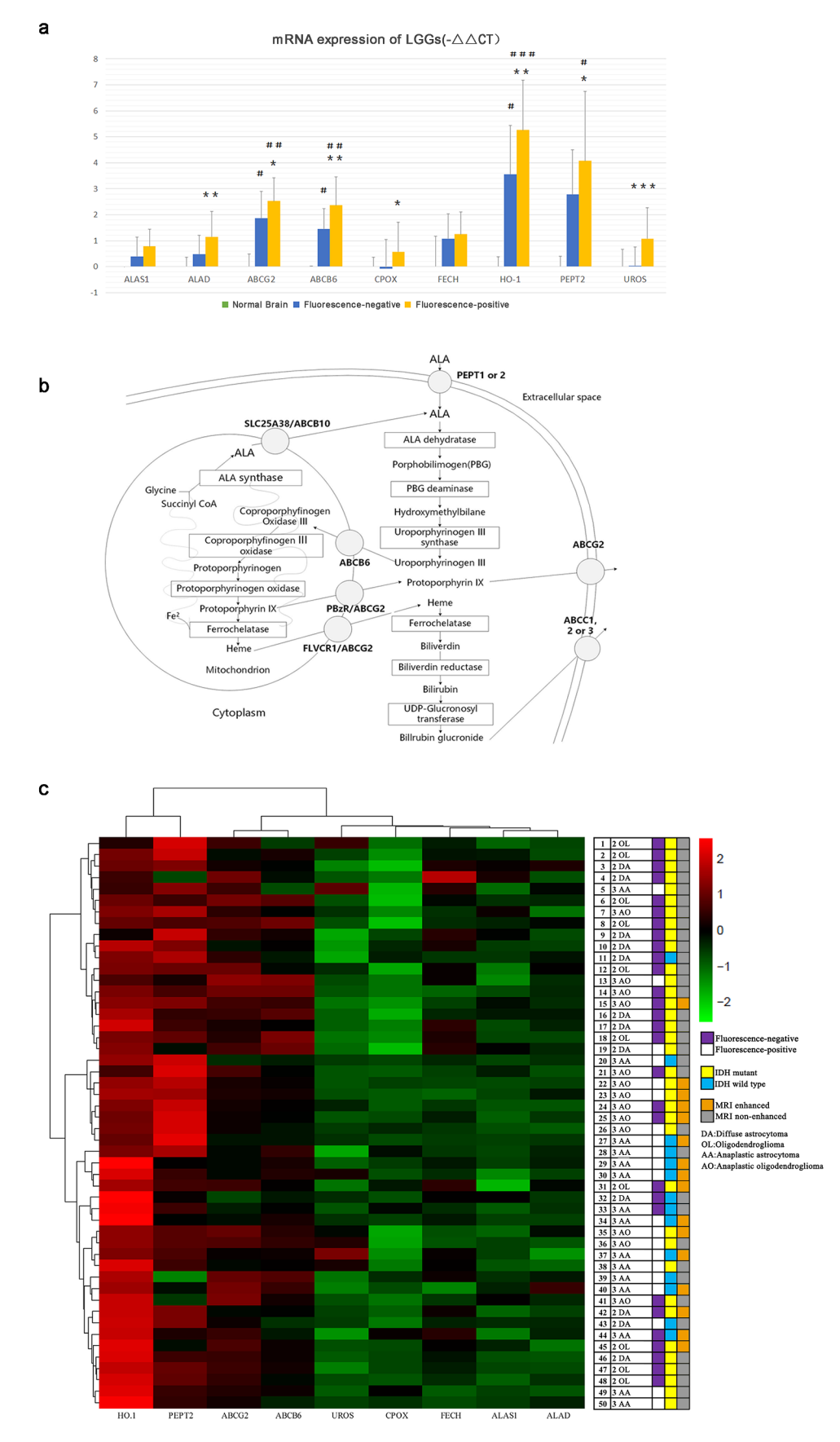
a
mRNA expression of LGGs(-△△CT)
ALAS1
ALAD
ABCG2
ABCB6
CPOX
FECH
HO-1
PEPT2
UROS
Normal Brain
Fluorescence-negative
Fluorescence-positive
b
ALA
PEPT1 or 2
Extracellular space
SLC25A38/ABCB10
ALA dehydratase
Porphobilimogen(PBG)
ALA synthase
Glycine
Succinyl CoA
PBG deaminase
Hydroxymethylbilane
Coproporphyfinogen Oxidase III
Uroporphyrinogen III synthase
Coproporphyfinogen III oxidase
ABCB6
Uroporphyrinogen III
ABCG2
Protoporphyrinogen
Protoporphyrinogen oxidase
Protoporphyrin IX
Fe2
PBzR/ABCG2
Heme
Ferrochelatase
ABCC1, 2 or 3
Biliverdin
FLVCR1/ABCG2
Biliverdin reductase
Mitochondrion
Bilirubin
Cytoplasm
UDP-Glucronosyl transferase
Billrubin glucronide
c
HO.1
PEPT2
ABCG2
ABCB6
UROS
CPOX
FECH
ALAS1
ALAD
Fluorescence-negative
Fluorescence-positive
IDH mutant
IDH wild type
MRI enhanced
MRI non-enhanced
DA:Diffuse astrocytoma
OL:Oligodendroglioma
AA:Anaplastic astrocytoma
AO:Anaplastic oligodendroglioma

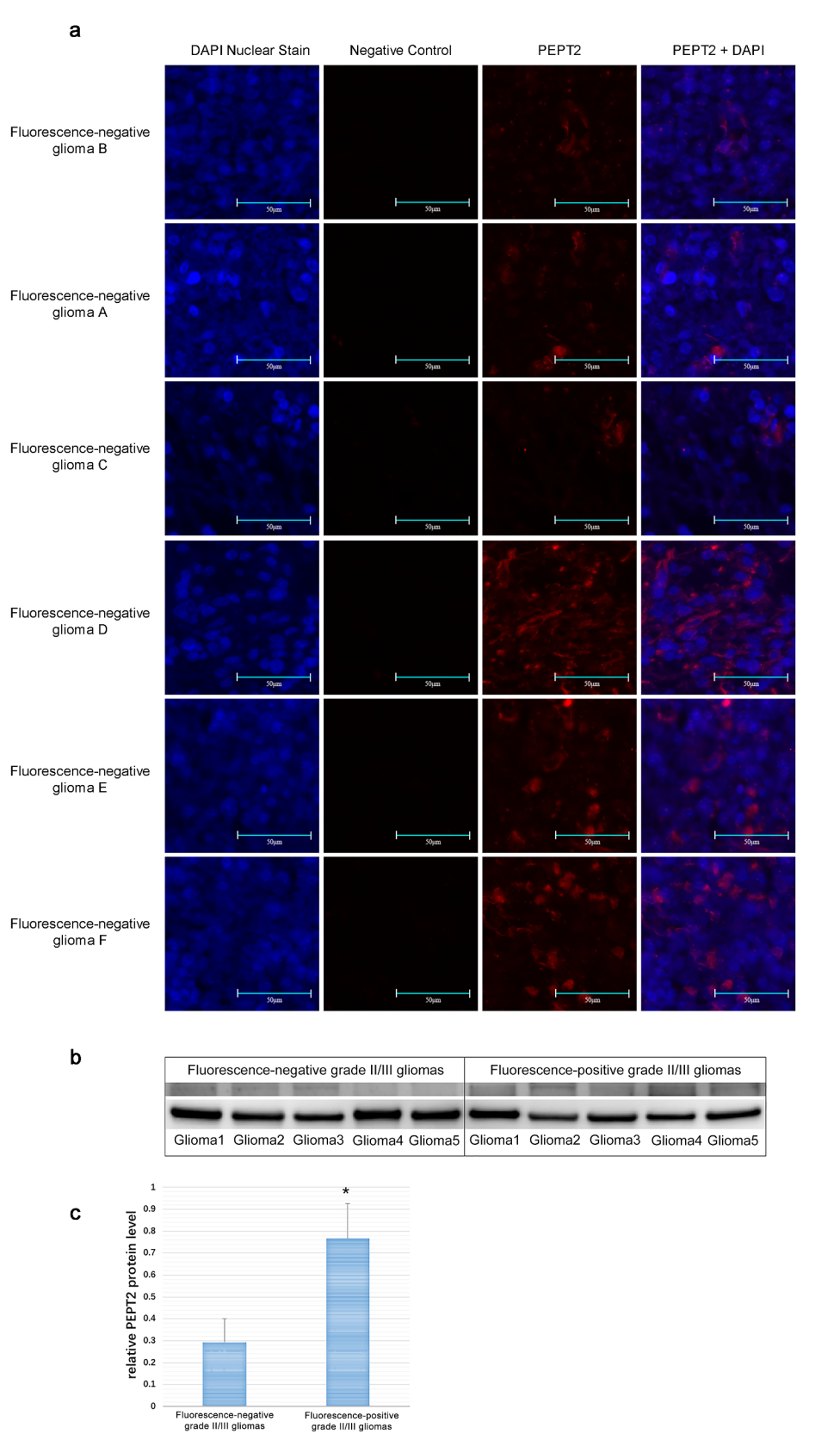
a
DAPI Nuclear Stain
Negative Control
PEPT2
PEPT2 + DAPI
Fluorescence-negative glioma B
Fluorescence-negative glioma A
Fluorescence-negative glioma C
Fluorescence-negative glioma D
Fluorescence-negative glioma E
Fluorescence-negative glioma F
50μm
b
Fluorescence-negative grade II/III gliomas
Fluorescence-positive grade II/III gliomas
Glioma1 Glioma2 Glioma3 Glioma4 Glioma5
Glioma1 Glioma2 Glioma3 Glioma4 Glioma5
c
relative PEPT2 protein level
0
0.1
0.2
0.3
0.4
0.5
0.6
0.7
0.8
0.9
1
*
Fluorescence-negative grade II/III gliomas
Fluorescence-positive grade II/III gliomas

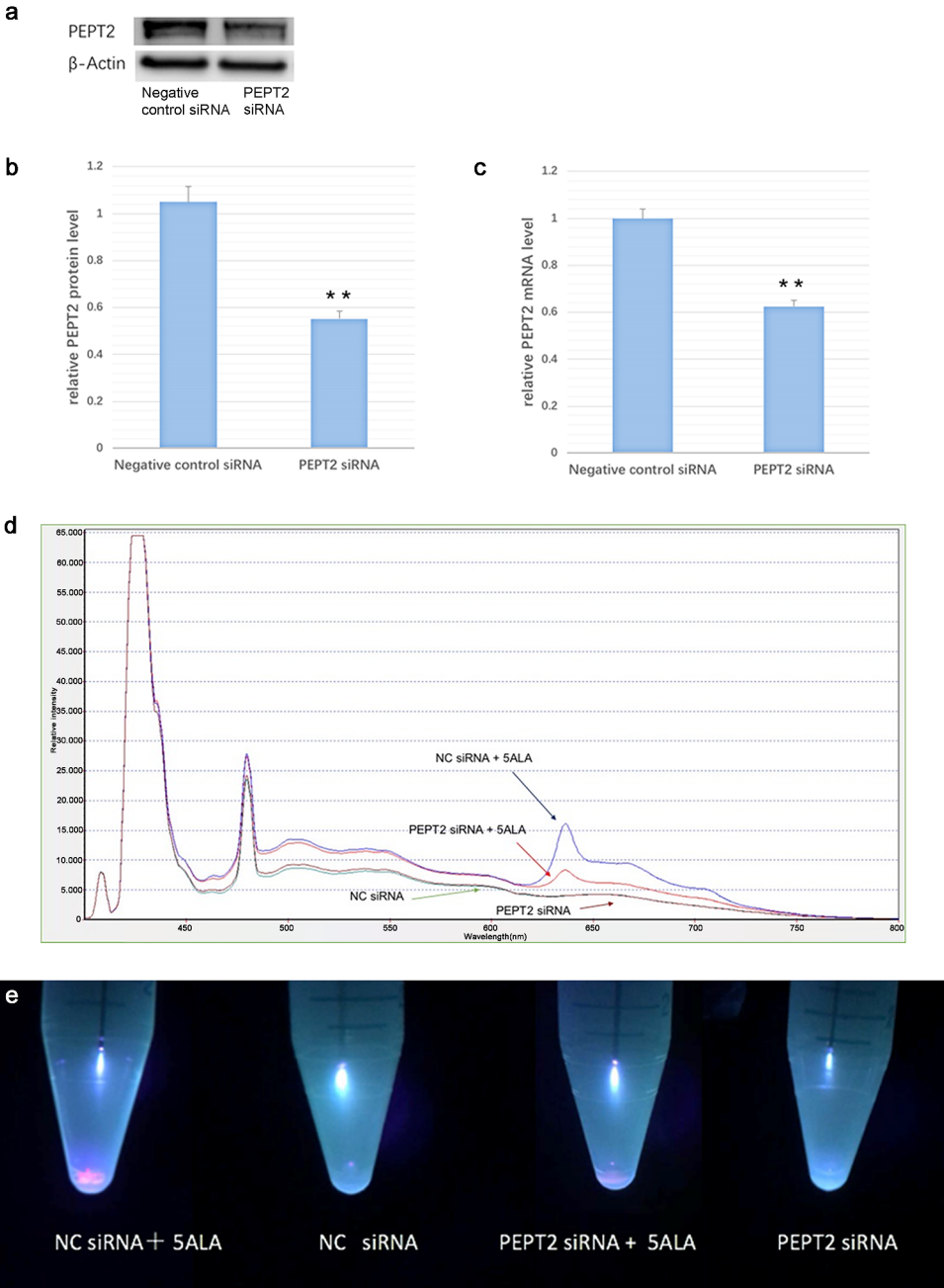
a
PEPT2
β-Actin
Negative control siRNA
PEPT2 siRNA
b
relative PEPT2 protein level
1.2
1
0.8
0.6
0.4
0.2
0
**
Negative control siRNA
PEPT2 siRNA
c
relative PEPT2 mRNA level
1.2
1
0.8
0.6
0.4
0.2
0
**
Negative control siRNA
PEPT2 siRNA
d
Relative Intensity
65.000
60.000
55.000
50.000
45.000
40.000
35.000
30.000
25.000
20.000
15.000
10.000
5.000
0
450
500
550
600
650
700
750
800
Wavelength(nm)
NC siRNA + 5ALA
PEPT2 siRNA + 5ALA
NC siRNA
PEPT2 siRNA
e
NC siRNA＋ 5ALA
NC siRNA
PEPT2 siRNA + 5ALA
PEPT2 siRNA